Monthly Notices
of the
ROYAL ASTRONOMICAL SOCIETY

MNRAS **493,** 1306–1316 (2020)
Advance Access publication 2020 February 11

doi:10.1093/mnras/staa371

The loss of the intracluster medium in globular clusters

W. Chantereau,[1]★ P. Biernacki,[2,3] M. Martig,[1] N. Bastian,[1] M. Salaris[1] and R. Teyssier[3]

[1]*Astrophysics Research Institute, Liverpool John Moores University, 146 Brownlow Hill, Liverpool L3 5RF, UK*
[2]*Kavli Institute for Cosmology & Institute of Astronomy, University of Cambridge, Madingley Road, Cambridge CB3 0HA, UK*
[3]*Center for Theoretical Astrophysics and Cosmology, Institute for Computational Science, University of Zurich, Winterthurerstrasse 190, CH-8057 Zurich, Switzerland*

Accepted 2020 February 5. Received 2019 December 20; in original form 2019 October 23

ABSTRACT

Stars in globular clusters (GCs) lose a non-negligible amount of mass during their post-main-sequence evolution. This material is then expected to build up a substantial intracluster medium (ICM) within the GC. However, the observed gas content in GCs is a couple of orders of magnitude below these expectations. Here, we follow the evolution of this stellar wind material through hydrodynamical simulations to attempt to reconcile theoretical predictions with observations. We test different mechanisms proposed in the literature to clear out the gas such as ram-pressure stripping by the motion of the GC in the Galactic halo medium and ionization by UV sources. We use the code RAMSES to run 3D hydrodynamical simulations to study for the first time, the ICM evolution within discretized multimass GC models including stellar winds and full radiative transfer. We find that the inclusion of both ram pressure and ionization is mandatory to explain why only a very low amount of ionized gas is observed in the core of GCs. The same mechanisms operating in ancient GCs that clear the gas could also be efficient at younger ages, meaning that young GCs would not be able to retain gas and form multiple generations of stars as assumed in many models to explain 'multiple populations'. However, this rapid clearing of gas is consistent with observations of young massive clusters.

Key words: hydrodynamics – methods: numerical – stars: mass-loss – stars: winds, outflows – ISM: evolution – globular clusters: general.

1 INTRODUCTION

Globular clusters (GCs) in the Galaxy tend to be old (9–13 Gyr) and massive (from $\sim 10^4$ up to $\sim 10^6$ $M_\odot$). They are located from a few kpc up to ∼100 kpc from the Galactic centre and they orbit the Galaxy in a few hundreds Myr (e.g. Odenkirchen et al. 1997). GCs contain hundreds to thousands of stars along their red giant branches (RGBs), which display significant mass-loss (also along the asymptotic giant branch to some extent). This mass is lost through mostly[1] slow winds (∼10–20 km s^{-1}, e.g. Mauas, Cacciari & Pasquini 2006; McDonald & van Loon 2007; Mészáros, Avrett & Dupree 2009), well below the central escape velocities of GCs (of the order of a few km s^{-1} up to ∼90 km $^{-1}$, e.g. Baumgardt & Hilker 2018). The mass lost by the whole stellar population of a massive GC ($\sim 10^6$ $M_\odot$) can be approximated by $\sim 10^{-6}$ $M_\odot$ yr^{-1} (e.g. McDonald & Zijlstra 2015). GCs cross the Galactic disc over time-scales of a few hundreds Myr, where they are subject to ram pressure which is efficient at stripping all their ICM (Tayler & Wood 1975; Roberts 1988). Thus, stellar winds contribute to build up a non-negligible, observable intracluster medium (ICM) of a few hundreds of $M_\odot$ between two Galactic disc crossings.

However, at odds with these theoretical considerations, to date there has been only a single certain detection of neutral ICM in GCs: M15 (NGC 7078) displays 0.3 $M_\odot$ of neutral hydrogen H I and a very low amount of dust (9×10^{-4} $M_\odot$) in its core (Evans et al. 2003; Boyer et al. 2006; van Loon et al. 2006). In addition, Freire et al. (2001) inferred from the plasma mass density detected in 47 Tuc (NGC 104) that it should contain a total mass of ∼0.1 $M_\odot$ of gas within its inner 2.5 pc. Recently, Abbate et al. (2018) calculate a total mass of gas in the inner 1 pc of 47 Tuc to be 0.023 ± 0.005 $M_\odot$. Other searches for H I, CO, and H α in GCs all lead to only observational upper limits often lower than 1 $M_\odot$ and as low as 10^{-5} $M_\odot$ (e.g. Roberts 1988; Smith et al. 1990; van Loon et al. 2006; Boyer et al. 2008; Matsunaga et al. 2008; Barmby et al. 2009; van Loon et al. 2009, and references therein).

Therefore, to explain the negligible amount of ICM observed in GCs, a mechanism to get rid of the gas with a time-scale much

★ E-mail: w.chantereau@ljmu.ac.uk

[1]Note, however, that fast outflows can also be found, but it represents a minority (Dupree, Smith & Strader 2009).

lower than a few hundreds Myr should be at work. Several processes have been proposed in the literature to explain this missing ICM. Coleman & Worden (1977) suggested that flaring activity from M-dwarf stars would help to clear the GC from its ICM, however, this process is subject to several uncertainties (e.g. mass-loss rates). Vandenberg (1978) suggested hot horizontal-branch stars to heat the ICM due to their UV radiation, but the main drawback is that these stars are not present in all GCs. Classical novae have been proposed as an internal clearing mechanism, however, novae are effective at clearing the ICM only in low-mass GCs ($\leq 10^5$ M$_\odot$, Scott & Durisen 1978; Moore & Bildsten 2011). Spergel (1991) and Yokoo & Fukue (1992) considered winds of pulsars and X-ray bursters, respectively, as gas removal mechanisms. However, if they are present in the stellar cluster, they are not effective enough to heat the ICM (McDonald & Zijlstra 2015). Thoul et al. (2002) briefly mentioned that the mass lost through winds could be recycled by accretion on to low-mass stars. Umbreit, Chatterjee & Rasio (2008) invoked stellar collisions to remove the gas from M15 on time-scales of $\sim 10^6$ yr. Finally, Dupree et al. (2009) suggested that stellar winds of RGB stars were fast enough to leave the cluster potential. However, most of the studies in the literature found that velocities of low-mass giant winds are rather low and range between a few and $\sim$20 km s^{-1} (e.g. Netzer & Elitzur 1993; Mauas et al. 2006; McDonald & van Loon 2007; Mészáros et al. 2009; Groenewegen 2014).

Frank & Gisler (1976) and Priestley, Ruffert & Salaris (2011) investigated the ram-pressure stripping of the ICM as the GC moves through the Galactic halo. However, Priestley et al. (2011) have shown with a hydrodynamical study[2] that this mechanism is sufficient to limit the amount of ICM to levels similar to what it is observed only within intermediate-mass GCs ($\sim 10^5$ M$_\odot$). Thus, an additional process is needed to explain observations in massive GCs ($\sim 10^6$ M$_\odot$). Recently, McDonald & Zijlstra (2015) investigated the UV radiation from cooling WDs and hot post-AGB stars in stellar clusters and they showed with a 1D model that the ICM of every GCs should be ionized,[3] and in turn, the ICM would expand beyond the GC's tidal radius and would escape its gravitational potential. However, in this case full hydrodynamic models would be mandatory to take into account different physical mechanisms at work and better describe e.g. the interplay between the ICM and the Galactic halo.

In this paper, we follow the different suggestions of Priestley et al. (2011) and McDonald & Zijlstra (2015) and test the effects of ram-pressure stripping by the motion of the stellar cluster in the Galactic halo medium and the inclusion of internal ionizing sources on the ICM evolution in GCs. We investigate these two mechanisms in intermediate-mass and massive GCs to propose a general solution to the lack of gas in GCs and explain all the observations. We use full 3D hydrodynamical simulations with the adaptive mesh refinement (AMR) code RAMSES to follow for the first time the ICM evolution within discretized multimass GC models[4] taking into account stellar winds, ionizing radiation, radiative heating, and radiative pressure. We present the code and the set-up of the two sets of simulations for typical intermediate-mass (Simu1, $\sim 10^5$ M$_\odot$) and a massive GC such as 47 Tuc (Simu2, $\sim 10^6$ M$_\odot$) in Section 2. We discuss the different effects of the ram-pressure stripping and ionization mechanisms on the ICM evolution in these GCs in Section 3. Finally, we summarize the results and discuss their implications in Section 4.

[2]They did not model full radiative transfer and took into account a discrete, orbiting stellar population in their simulations at low resolution only as exploratory stages.

[3]Note that it has also been shown with 3D hydrodynamical models that photoionization has a great impact on stellar formation in young star clusters (Geen et al. 2015; Gavagnin et al. 2017).

[4]The stellar population of the cluster is represented by modelling each individual star with different masses and orbiting in the cluster potential.

2 SIMULATION SET-UP

We have performed 3D simulations using the AMR code RAMSES (Teyssier 2002), which uses the second-order, unsplit Godunov scheme to solve the Euler equations. The dynamical evolution of the stars employs the adaptive particle-mesh solver with cloud-in-cell interpolation. We do not allow new stars to form and we do not include any supernova feedback modelling, as we do not expect any star formation or stars to explode during the time of evolution of our simulations. We do not model any external potential that would come from the halo/Galaxy. The cooling of gas follows the prescription given by Sutherland & Dopita (1993) for radiative cooling of gas for H, He, and metal lines if the gas is hotter than 10^4 K and from metal fine-structure cooling processes at lower temperatures. We advect the metallicity in the form of a passive scalar and we follow it in each cell. A temperature floor is introduced at 50 K. It prevents the gas from artificial fragmentation by matching the corresponding Jeans length to our adopted resolution. The mesh refinement strategy we have adopted for all our simulations is a quasi-Lagrangian approach, where cells are refined once their mass exceed 1.25×10^{-4} M$_\odot$. The maximum spatial resolution achieved by our simulations is 0.098–0.146 pc for a box length of 100–150 pc for the first and the second set of simulations, respectively.[5] The minimum and maximum levels of refinement are 8 and 10, respectively. We model at high resolution for each simulation individual stars orbiting in the cluster potential. We use as a boundary condition free outflow. In simulations where the full radiative transfer is used (RAMSES-RT, Rosdahl et al. 2013; Rosdahl & Teyssier 2015), we use the non-equilibrium cooling. As in Rosdahl et al. (2015), we group the photons into five bins, with the same energies, which we list in Table 1. The energy fraction per photon group follows the average spectral energy distribution (SED) of a hot post-AGB star (cf. next section and Section 3.2).

2.1 Initial conditions

In this study, we follow the suggestions of Priestley et al. (2011) and McDonald & Zijlstra (2015) and investigate the effects of the ram-pressure and ionization mechanisms on typical intermediate-mass (Simu1, 10^5 M$_\odot$) and a massive GC such as 47 Tuc (Simu2, $\sim 10^6$ M$_\odot$). We choose and present below initial conditions for massive GCs similar to what is used in McDonald & Zijlstra (2015) and for typical intermediate-mass GCs similar to what is used in Priestley et al. (2011).

We reproduce the stellar structure of globular clusters with discretized multimass models with the LIMEPY code (Gieles & Zocchi 2015), which aims at describing the phase-space density of stars in tidally limited and mass-segregated star clusters. The initial, non-rotating stellar distribution follows a King profile with a central gravitational potential of 7 (King 1966), similar to the value used in Priestley et al. (2011) of 7.5.

[5]The box radius is larger than the typical tidal radius of intermediate-mass GCs (first set of simulations) and than massive GCs (second set of simulations) to not lose any information (e.g. $r_t \sim 52.5$ pc for 47 Tuc, de Boer et al. 2019)

Table 1. Properties of the photon groups used in the radiative transfer simulations. The energy intervals defined by the groups are indicated by ϵ_0 and ϵ_1. $\sigma_{\rm H\,I}$, $\sigma_{\rm He\,I}$, and $\sigma_{\rm He\,II}$ denote the cross-sections for ionization of hydrogen and helium, respectively. $\tilde{\kappa}$ is the dust opacity. $f_{\gamma,\,\rm i}$ is the reduced flux of the radiation of the group i (describing the directionality of the radiation).

Photon group	ϵ_0 (eV)	ϵ_1 (eV)	$\sigma_{\rm H\,I}$ (cm^2)	$\sigma_{\rm He\,I}$ (cm^2)	$\sigma_{\rm He\,II}$ (cm^2)	$\tilde{\kappa}$ (cm^2 g^{-1})	$f_{\gamma,\,\rm i}$
IR	0.10	1.00	0	0	0	10	0.2289
Opt	1.00	13.60	0	0	0	1000	0.3759
$\rm UV_{H\,I}$	13.60	24.59	3.3×10^{-18}	0	0	1000	0.0829
$\rm UV_{He\,I}$	24.59	54.42	6.3×10^{-19}	4.8×10^{-18}	0	1000	0.0695
$\rm UV_{He\,II}$	54.42	∞	9.9×10^{-20}	1.4×10^{-19}	1.3×10^{-18}	1000	0.1243

Table 2. Main characteristics of the different simulations. $M_{\rm cluster}$ is the mass of the stellar cluster (M$_\odot$); $V_{\rm cluster}$ the velocity of the cluster in the halo (km s^{-1}); $\dot{M}_*$ the total cluster stellar mass-loss rate (M$_\odot$ yr^{-1}); $T_{\rm winds}$ the temperature of the stellar winds (K); $T_{\rm halo}$ the temperature of the halo gas (K); $\rho_{\rm halo}$ the halo gas density (cm^{-3}); the UV flux (s^{-1}, $\lambda < 912$ Å;, i.e. $\epsilon > 13.6$ eV).

ID	$M_{\rm cluster}$ (M$_\odot$)	$V_{\rm cluster}$ (km s^{-1})	$\dot{M}_*$ (M$_\odot$ yr^{-1})	$T_{\rm winds}$ (K)	$T_{\rm halo}$ (K)	$\rho_{\rm halo}$ (cm^{-3})	UV flux (s^{-1})
Simu1A	10^5	0	3.2×10^{-7}	6000	$10^{5.5}$	6×10^{-4}	0
Simu1B	10^5	200	3.2×10^{-7}	6000	$10^{5.5}$	6×10^{-4}	0
Simu1C	10^5	200	3.2×10^{-7}	6000	$10^{5.5}$	6×10^{-3}	0
Simu1D	10^5	200	3.2×10^{-7}	4000	$10^{5.5}$	6×10^{-4}	0
Simu2A	10^6	200	2.8×10^{-6}	6000	$10^{5.5}$	7×10^{-3}	0
Simu2B	10^6	200	2.8×10^{-6}	6000	$10^{5.5}$	7×10^{-3}	5.7×10^{48}
Simu2C	10^6	200	2.8×10^{-6}	6000	$10^{5.5}$	1×10^{-4}	0
Simu2D	10^6	200	2.8×10^{-6}	6000	$10^{5.5}$	1×10^{-4}	5.7×10^{48}
Simu2E	10^6	200	2.8×10^{-6}	6000	$10^{5.5}$	7×10^{-3}	2.43×10^{47}

The properties of the two sets of simulations are presented in Table 2.

The intermediate-mass GC is a general case (we do not associate it to a particular GC), thus we choose that its stellar population follows a mass function with a slope α of -2.35 down to $\sim$0.1 M$_\odot$ (Salpeter 1955). Since we chose 47 Tuc as the massive GC, the stellar population follows its global mass function with $\alpha = -0.53$ down to $\sim$0.1 M$_\odot$ (Baumgardt & Hilker 2018). Thus we have more than $\sim$500 000 and $\sim$3000 000 stars in our 10^5 and 10^6 M$_\odot$ GCs, respectively. This difference between the two mass functions has only a negligible impact on the stellar structure of our cluster and does not have any effect on our results.

The initial conditions of our simulations feature a gas grid which is filled with a uniform medium at $10^{5.5}$ K. The medium density in the first set of simulations is 6×10^{-4} cm^{-3} ($\sim 10^{-27}$ g cm^{-3}) in agreement with the properties of a hot Galactic halo medium (Spitzer 1956) and similar to what is used in Priestley et al. (2011). The medium density in the second set of simulations is 7×10^{-3} cm^{-3} in agreement with the properties of the Galactic halo medium where the globular cluster 47 Tuc evolves (Taylor & Cordes 1993; McDonald & Zijlstra 2015). We fix the metallicity to an initial value of $Z = 0.002$, like in Priestley et al. (2011), for the gas and stars, we keep this value between the different sets of simulations since the metallicity of 47 Tuc is close ($Z \sim 0.004$, depending on the alpha enhancement).

2.2 Ionizing source

We do not include any UV radiation while modelling the intermediate-mass GC in the first set of simulations. In the second set of simulations (Simu2, massive GCs such as 47 Tuc, $\sim 10^6$ M$_\odot$), we follow the suggestion of McDonald & Zijlstra (2015) to investigate the effect of UV radiation from post-AGB stars. We include ionizing radiation from a source (i.e. radiative heating and radiative pressure) in several simulations of this set (*Simu2B, Simu2D*, and *Simu2E*). To take into account this source, we need to provide an SED with its properties.

We took as a typical post-AGB star for a massive GC such as 47 Tuc, a model with an initial main-sequence mass of 0.93 M$_\odot$ at [Fe/H] $= -0.72$ with [α/Fe] $= +0.4$, which has an age of 12.4 Gyr at the RGB-tip and a current mass of $\sim$0.59 M$_\odot$ (STAREVOL, Lagarde et al. 2012). Then, to estimate the ionizing photon rate of this source, we determine the properties of this star (temperature and luminosity) by averaging by the time spent in the region where a hot post-AGB star/cooling WD is supposed to fully ionize the ICM of 47 Tuc ($T_{\rm eff} > 14\,000$ K and $L > 1$ L$_\odot$, McDonald & Zijlstra 2015). This ionizing source has a resulting very high mean temperature of $\sim$95 000 K and a luminosity of $\sim 10^{3.57}$ L$_\odot$, it is then a hot post-AGB star which has still not entered the cooling sequence. We then create an SED of a blackbody with this effective temperature. It gives us an average of 5.7×10^{48} ionizing photons s^{-1} ($\lambda < 912$ Å). This value is an order of magnitude higher than the value from the model from McDonald & Zijlstra (2015; 2.43×10^{47} s^{-1}); it allows us to maximize the continuous ionizing photons rate and thus test the limit of this ionizing mechanism. However, both ionizing photon rates are already a few orders of magnitude higher than the rate needed to fully ionize the ICM of 47 Tuc (1.6×10^{44} photons s^{-1}, McDonald & Zijlstra 2015). Thus, we would expect that the difference between these values has only a negligible effect on the results of the simulations. The source is then associated with one of the star particle in the simulation, which displays a mass typical of a post-AGB in this GC. In our simulations, it is initially located in the cube at the position $X, Y, Z = -0.066, -0.04, -0.32$ in pc, thus it is near the centre of the GC.

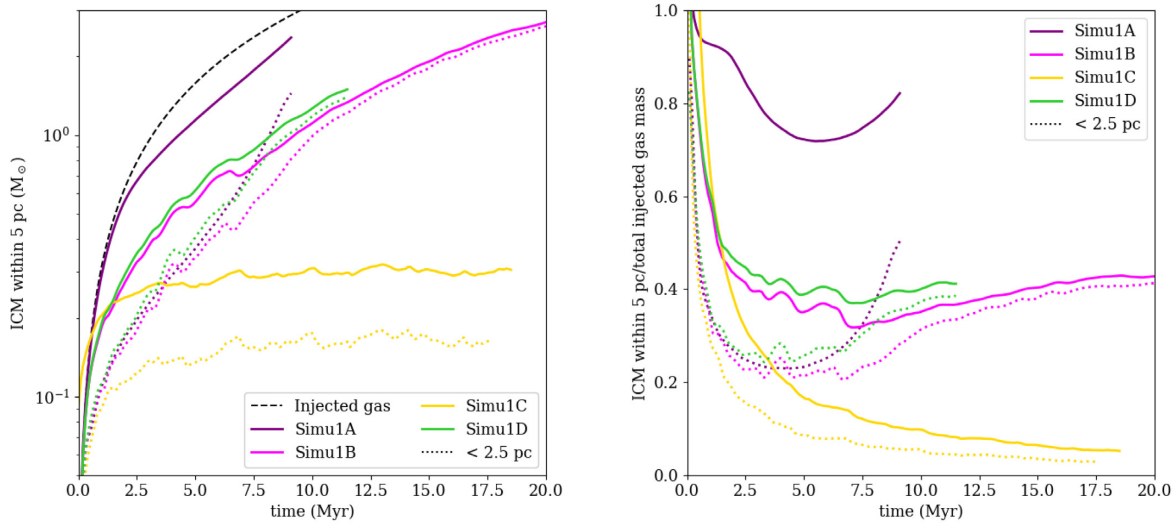

Figure 1. *Left:* ICM mass within 5 pc and the central part of 2.5 pc (solid and dotted lines, respectively) for the first set of simulations as a function of time. *Right:* ratio of the ICM mass within 5 pc over the total mass injected by stellar winds for the first set of simulations as a function of time.

2.3 Stellar winds

Stellar winds are expected to produce radially symmetric outflows. This is true if the stellar rotation is minimal and if the star is static with respect to the ICM. Stellar winds are in general a complicated function of stellar mass and metallicity and vary with the age of a star. The gas ejected by a star would be characterized by its mass, temperature, and velocity. Keeping these parameters in mind, we introduce a simple stellar wind model, which can mimic the true stellar wind in hydrodynamical simulations.

Ideally, the gas injected by the star into a grid should be spread spherically around the star. In case of the AMR simulations, one would be required to find all nearby grid elements and inject the right mass, momentum, and pressure taking into account their size and distance. Here, we propose a simpler approach, which statistically gives the same result. At each time-step, we inject the aforementioned quantities *only* in the cell in which the star resides with a randomly generated velocity vector and a magnitude corresponding to the chosen wind speed. It is apparent that enough repetitions of these injections would lead to spherical distribution of the gas around a star (whose mass is reduced by the amount of mass injected into a cell). To make it correct in the global frame of reference, we add the velocity of the parent star to the velocity of its injected gas. For simplicity, we do not include the time dependence on the wind injection rate, as our simulations were not run over periods in which the wind rate could change significantly.

Here, we consider only the mass-loss of RGB stars, since the number of AGB stars is negligible compared to the number of RGB stars. To summarize, only star particles on the upper RGB ($\log\left(\frac{L}{L_\odot}\right) \gtrsim 2.0$, as mass-loss occurs near the very end of the RGB evolutionary stage) inject gas to the grid in which it resides with constant rate, velocity, temperature, and metallicity.

In the first set of simulations (Simu1, intermediate-mass GC), we adjust the mass-loss rate per star to get a total mass-loss rate ($\sim 3.2 \times 10^{-7}$ $M_\odot$ yr^{-1}) similar to what is used in Priestley et al. (2011). In the second set of simulations (Simu2, massive GC), we use an average mass-loss computed with the stellar evolution code STAREVOL for a 0.93 $M_\odot$ star at [Fe/H] $= -0.72$ with [α/Fe] $= +0.4$ (12.4 Gyr at the RGB-tip). The mean value of the mass-loss rate along the RGB is 1.3×10^{-9} $M_\odot$ yr^{-1} in our case (mass-loss parameter $\eta = 0.5$, Reimers 1975), and the total mass-loss rate of the stellar cluster is then $\sim 2.8 \times 10^{-6}$ $M_\odot$ yr^{-1}, similar to what is used in McDonald & Zijlstra (2015). We choose a typical value for the wind velocity of 20 km s^{-1}, the temperature of the wind is chosen to be the effective temperature of the progenitor. We choose 6000 K, which is an upper limit of the stellar $T_{\rm eff}$ of RGB stars in metal-poor clusters (we will also test 4000 K which is typical of stars of the upper RGB close to the tip in more metal rich globular clusters, Simu1D, see Table 2). Finally each chosen star injects gas with $Z = 0.002$, metallicity used for the simulations in Priestley et al. (2011) and close to the metallicity of 47 Tuc ($Z \sim 0.003$, depending on the alpha enhancement).

3 RESULTS

3.1 Intermediate-mass GC – Simu1

Priestley et al. (2011) showed that the motion of typical intermediate-mass GCs through the Galactic halo medium reduces the ICM content due to ram-pressure stripping. Thus, we discuss a first set of models to test the effect of the different parameters and processes, especially the ram-pressure stripping mechanism, on the ICM evolution in typical intermediate-mass GCs. These parameters are the velocity of the GC, the halo medium density, and the temperature of the stellar winds.[6] We list in Table 2, the different simulations presented in this paper with their main characteristics. More details are presented in the following sections. We run each simulation until the mass of the ICM within 5 pc over the total stellar mass-loss (cf. Fig. 1, right-hand panel) reaches a stable behaviour (e.g. gas accumulation) or an asymptotic behaviour indicating a steady state. We choose this radius as it is a good approximation for the half-mass radius of globular clusters in general (Baumgardt & Hilker 2018; de Boer et al. 2019). Indeed, most of the observations

[6]We did not investigate the effect of the stellar mass-loss rate parameter in this study and used canonical values which are favoured in the literature. However, it can have an effect on the results (as discussed in Priestley et al. 2011).

to detect the ICM in GCs are focused on their core region and are done within this radius.

3.1.1 Simu1A: control simulation

We use *Simu1A* as a control simulation for this set, we include hot stellar winds in a GC at rest in the halo where no ionizing source is present (cf. Table 2).

We show the mass accumulated within 5 pc as a function of time for our different simulations of the first set in Fig. 1.[7] After ∼5 Myr, most of the ICM gas cools and sinks to the centre of the cluster (Fig. 1), which means that the energy from the stellar winds is not sufficient to heat and expand the gas beyond the half-mass radius (see Fig. 2). To summarize, in this simulation nearly all the ICM injected into the GC by stellar winds is retained, including a significant amount in the cluster centre (we choose for every simulation an arbitrary radius of 2.5 pc for the central region). We summarize the ICM mass in this central area and within 5 pc at 5 Myr for all the simulations in Table 3.

3.1.2 Simu1B: with ram-pressure stripping

From now on, in all the simulations, the stellar cluster is at rest in the centre of the simulation volume (GC's frame of reference) and we introduce a continuous flow of the halo medium in the x-direction. We use an orbital velocity of the GC of 200 km s^{-1}. To do that, we assume that the gas in each cell of the simulation has a velocity of $v_x = 200$ km s^{-1} at $t = 0$. The other parameters are identical to the ones used in *Simu1A*, i.e. we include hot stellar winds and no ionizing source is present.

We see in Fig. 2 that the GC is stripped in its central region (∼3 pc). The motion of the GC through the ambient environment creates a bow shock with a temperature at $\sim 10^6$ K. If we now take a look at Fig. 1, right-hand panel, the flattening of the curve means that there is equilibrium between the ram-pressure and the gravity forces. Despite a large part of the gas being stripped via the ram-pressure effect (more than half of the total injected gas already at 20 Myr), most of the ICM is located in the core region of 2.5 pc (> 96 per cent of the mass), the rest is located in the tail of the GC, composed of the stripped material (Fig. 2). Therefore, even if the ram-pressure stripping allows to get rid of a large part of the ICM, most of the remaining gas cools and sinks in the central region of the cluster and one needs an additional mechanism to limit the amount of ICM to levels similar to what it is observed.

3.1.3 Simu1C: denser halo

In this simulation, we test if the ram pressure can strip all the ICM by increasing the density of the ambient medium. We include hot stellar winds, no ionizing source is present and the halo is denser by one order of magnitude ($\rho_{\rm halo} = 6 \times 10^{-3}$ cm^{-3}).

We see in Fig. 2 that most of the gas is stripped away already at 5 Myr, but not all of it (down to a radius of ∼0.8 pc). Only 0.3 M$_\odot$ is retained within the inner 5 pc of the cluster and only ∼0.12 M$_\odot$ in the central region of the cluster (within 2.5 pc). This value is compatible with observational upper limits found in GCs often lower than 1 M$_\odot$ (e.g. Roberts 1988; Smith et al. 1990; van Loon et al. 2006; Boyer et al. 2008; Matsunaga et al. 2008; Barmby et al. 2009; van Loon et al. 2009).

We can conclude that the ram-pressure stripping due to the orbital motion of the GC in a rather dense halo medium is an efficient mechanism to limit the ICM in the central part of the stellar cluster at levels similar to observations.

3.1.4 Simu1D: cool stellar winds

The temperature of the winds we used so far is 6000 K, which corresponds to effective temperature of RGB stars in the metal-poor regime of Galactic GCs. The temperature of the wind and its velocity contribute to the energy of the cell in which the star resides. Thus, it might have an effect on our result since it changes the resulting pressure. In this simulation, we use a cooler wind temperature of 4000 K, which is typical of the effective temperature of stars on the upper RGB close to the tip in metal-rich globular clusters, to test the effect of this parameter. We do not include any ionizing source and the GC is moving in a tenuous halo as in *Simu1B*.

As expected, the decreased energy from the winds' lower temperature leads to similar results for the ICM values within the inner 5 pc but the mass accumulated is slightly larger than in *Simu1B* (Fig. 1). We have tested here two rather extreme values of the temperature spanning a range of 2000 K and we conclude that the temperature of the winds has only a limited effect.

3.2 Massive GC – Simu2

We have shown that for typical intermediate-mass GCs, a dense medium is necessary to maintain the ICM down to levels similar to observational limits. Now, we look at massive GCs and we specifically focus on 47 Tuc (1.1×10^6 M$_\odot$, McDonald & Zijlstra 2015). We expect that it will be more difficult to limit the ICM in massive GCs since the stellar mass-loss is higher and they have a deeper gravitational potential.

We run several simulations to test the effect of different parameters on the gas evolution within massive stellar cluster, these parameters are the UV flux from ionizing sources and the halo medium density.

3.2.1 Simu2A: control simulation

In this simulation, as in the previous set we include hot stellar winds and no ionizing source is present. However, the halo density is higher (7×10^{-3} cm^{-3}) in agreement with the properties of the Galactic halo medium where the globular cluster 47 Tuc evolves (Taylor & Cordes 1993; McDonald & Zijlstra 2015). This density is similar to what is used in *Simu1C* and was the key parameter to efficiently strip through ram pressure most of the stellar cluster's ICM in a typical intermediate-mass GC to levels similar to observations. We use *Simu2A* as a control simulation for this set.

The gas from the stellar winds[8] quickly cools and sinks into the centre of the cluster. There is 6.6 M$_\odot$ of gas within 2.5 pc after only 10 Myr and 6.8 M$_\odot$ within 5 pc, meaning that most of the gas left is located in the very central region of the cluster (Fig. 3). This is also seen in Fig. 4 (top panel) and Fig. 5, where we see that the GC is nearly entirely stripped, but the gas in the very centre is dense and cool.

[7] It is worth noting that all the mass injected through stellar winds is done within the inner 5 pc of the cluster.

[8] It is worth noting that most of the mass injected through stellar winds is done within the inner 5 pc of the cluster.

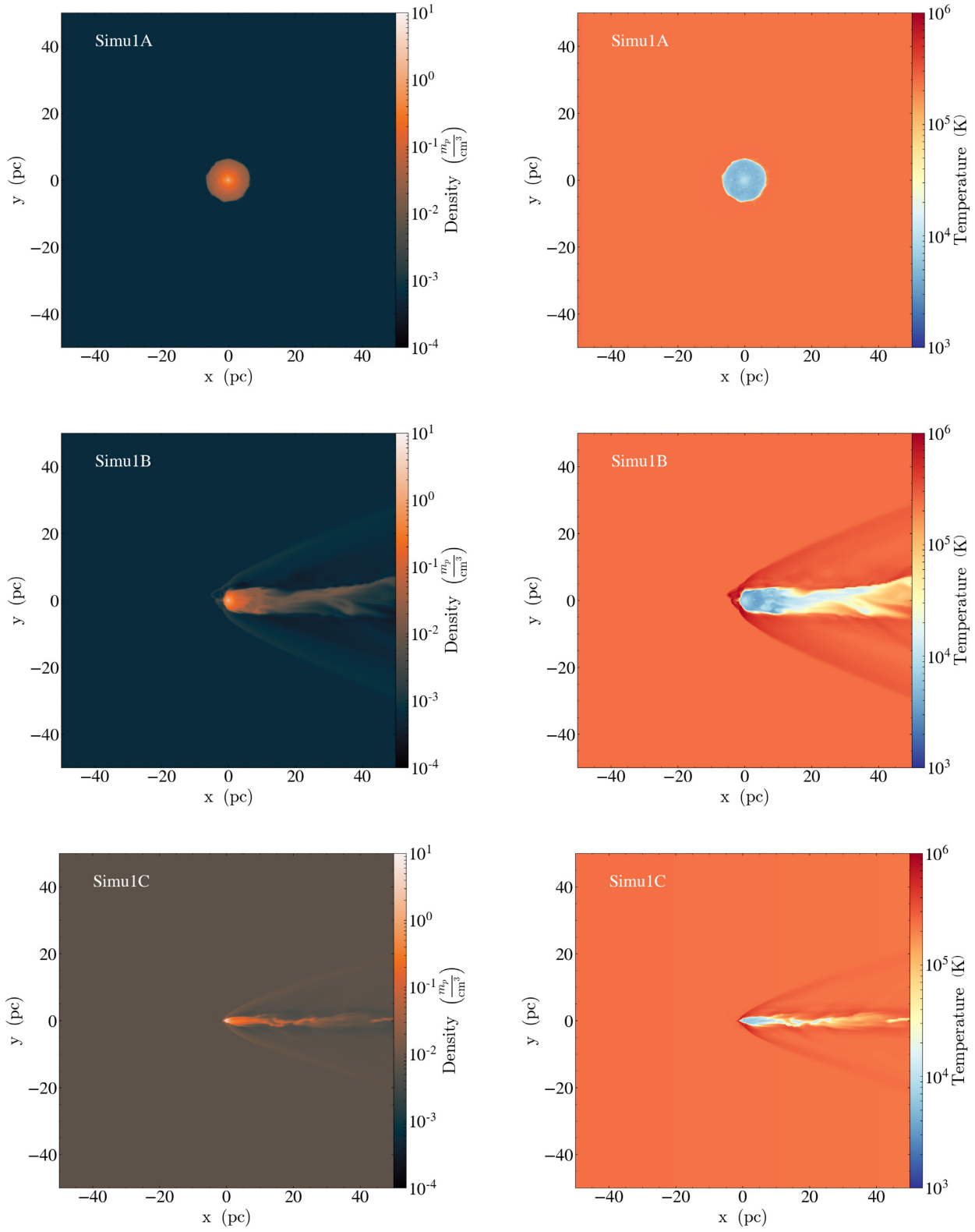

Figure 2. Snapshots at 5 Myr displaying the density (left) and temperature (right) maps of simulations *Simu1A*, *Simu1B*, and *Simu1C* (from top to bottom, respectively).

Table 3. ICM mass ($M_\odot$) within the centre (2.5 pc) and the typical cluster's half-mass radius (5 pc) of the different simulations at 5 Myr. M_{winds} is the total mass lost by stellar winds at 5 Myr.

Simulation	2.5 pc ($M_\odot$)	5 pc ($M_\odot$)
M_{winds}	–	1.58
Simu1A (control simulation)	0.37	1.14
Simu1B (with ram-pressure stripping)	0.34	0.55
Simu1C (denser halo)	0.12	0.26
Simu1D (cool stellar winds)	0.40	0.61
M_{winds}	–	14.0
Simu2A (control simulation)	3.30	3.49
Simu2B (UV ionizing flux)	0.26	0.56
Simu2C (tenuous halo)	8.48	8.90
Simu2D (tenuous halo and UV ionizing flux)	0.13	0.42
Simu2E (lower UV ionizing flux)	0.26	0.56

Thus, even if ram-pressure stripping allows to get rid of a large part of the gas[9] (more than 70 per cent of the total injected gas, Fig. 3, right-hand panel), the remaining part builds up a non-negligible ICM and is located in the very central region of the cluster.

3.2.2 *Simu2B: UV ionizing flux*

McDonald & Zijlstra (2015) have shown that UV radiation from hot post-AGB stars and cooling white dwarfs of 47 Tuc can keep its ICM ionized. In turn, this thermalized ICM will expand well beyond the half-mass radius. To test this, we add a post-AGB star as ionizing source in our simulation (see Section 2 for more details on the ionizing source). We include hot stellar winds and consider a dense halo environment.

As we can see in Fig. 4, second panel, and in more details in Fig. 5, the density in the centre of the cluster at 5 Myr is lower, up to two orders of magnitude, compared to the case where there is no ionizing source (*Simu2A*). This is due to the radiative heating and pressure of the gas from the ionizing source allowing the gas to expand quickly outwards (the ICM is completely ionized). In this case, the mass accumulated within its 5 pc reaches quickly (∼2 Myr) an asymptotic value of 0.6 $M_\odot$. In the centre of the cluster, i.e. 2.5 and 1 pc, this value is as low as ∼0.26 and ∼0.075 $M_\odot$, respectively. We expect about 11.2 $M_\odot$ of material lost by the stellar winds over 4 Myr within the inner 5 pc of the cluster. It means that 10.6 $M_\odot$ is located well beyond the half-mass radius of the cluster at 4 Myr (∼95 per cent of the total stellar mass-loss).

It confirms the results of McDonald & Zijlstra (2015) who predicted that ∼11.3 $M_\odot$ of ICM within 47 Tuc should be cleared over ∼4 Myr. In addition, it is in agreement with Freire et al. (2001) and McDonald & Zijlstra (2015) who claimed that all the gas left within 47 Tuc should be completely ionized. Finally, these results are similar to what was found by Freire et al. (2001) who reported a possible total ICM mass of ∼0.1 $M_\odot$ of gas within the inner 2.5 pc (0.26 $M_\odot$ in our case) and Abbate et al. (2018) calculated a total mass of gas in the inner 1 pc of 47 Tuc of 0.023 ± 0.005 $M_\odot$ (0.075 $M_\odot$ in our case).

We compare our results with observations at ∼7 Myr in our simulation whereas 47 Tuc crossed the Galactic disc around 30 Myr ago (Gillett et al. 1988). However, the ICM within the inner 5 and 2.5 pc reached a steady state (Fig. 3, right-hand panel), thus we do not expect differences between 7 and 30 Myr.

3.2.3 *Simu2C: tenuous halo*

We have shown in the case of typical intermediate-mass GCs that the halo density is a key parameter for the ICM ram-pressure stripping. We used in *Simu2A* and *Simu2B*, a high halo density which corresponds to 47 Tuc's environment (∼7.4 kpc from the Galactic centre). However, the halo density decreases quickly as a function of the distance from the Galactic centre. Thus, here we aim to also test the effect of ram-pressure stripping in massive clusters evolving in a tenuous environment, i.e. that would orbit further away from the Galactic centre.[10] It allows us to provide predictions for a broad range of stellar cluster's properties. 47 Tuc is a GC located at ∼7.4 kpc from the Galactic centre. If we assume a β-model as the gas density profile for the Galactic halo (Miller & Bregman 2013), then a halo density of ∼2 orders of magnitude lower to the one we used for 47 Tuc (previous simulations *Simu2A* and *Simu2B*) corresponds to a distance from the Galactic centre of ∼64 kpc. We then choose in this simulation a density of ∼2 orders of magnitude lower than before for the halo (1×10^{-4} cm^{-3}) to simulate a stellar cluster located at ∼64 kpc from the Galactic centre. We include hot stellar winds and no ionizing source is present in this simulation.

As in *Simu2A*, the gas quickly cools and most of it sinks into the centre of the cluster (Figs 3–5). The lower halo density compared to the one used in *Simu2A* limits logically the ram-pressure mechanism and the gas retained within the inner 5 pc of the cluster is more important. Most of the stellar winds are retained to form a 12.6 $M_\odot$ ICM within the inner 5 pc at 7 Myr (+160 per cent compared to *Simu2A*).

3.2.4 *Simu2D: tenuous halo and UV ionizing flux*

In this simulation, we test the effect of ram-pressure stripping and ionization in massive clusters evolving in a tenuous environment. The parameters are identical to the ones used in *Simu2C*, i.e. we include hot stellar winds and we choose a low density halo, however, we also include an ionizing source (same source as in *Simu2B*).

As we can see in Fig. 3, due to the very low initial gas density, there is less gas in the cluster centre compared to *Simu2B*. There is an ICM mass of 0.26 and 0.13 $M_\odot$ in the central region in *Simu2B* and *Simu2D*, respectively. The ICM mass is also very low in the half-mass radius region at 7 Myr (∼0.4 $M_\odot$).

Most of the studies to determine the ICM mass focus on the cluster centre (1–2.5 pc), thus we find low values of ICM in the cluster centre (0.026 and 0.13 $M_\odot$ at 1 and 2.5 pc, respectively) similar to what it is observed.

In this simulation, we have shown that massive clusters located far from the Galactic centre display similar ICM values in their core compared to GCs evolving close to the Galactic centre like 47 Tuc.

3.2.5 *Simu2E: lower UV ionizing flux*

McDonald & Zijlstra (2015) proposed an ionizing photon rate lower by one order of magnitude than the one we used in our simulation, their UV flux from model ($\lambda < 912$ Å) being 2.43×10^{47} s^{-1}. To numerically model their work and test their prediction, we run

[9] 47 Tuc crossed the Galactic disc around 30 Myr ago (Gillett et al. 1988), thus we would expect the stellar winds to contribute to about 84 $M_\odot$ to build up the ICM within the inner 5 pc.

[10] We assume here circular orbits for GCs.

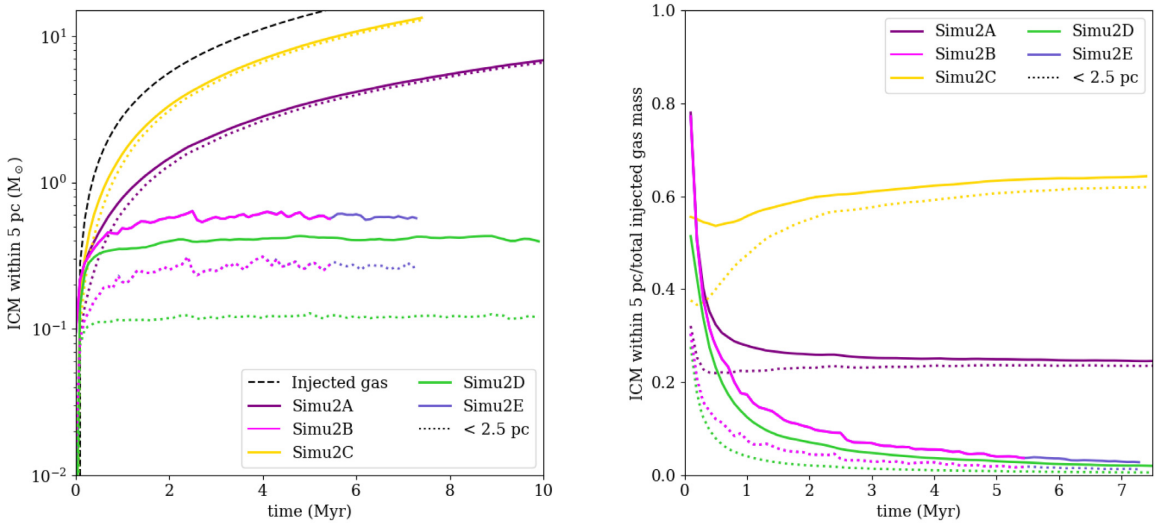

Figure 3. *Left:* ICM mass within 5 pc and the central part of 2.5 pc (solid and dotted lines, respectively) for the second set of simulations as a function of time. *Right:* ratio of the ICM mass within 5 pc over the total mass injected by stellar winds for the second set of simulations as a function of time.

the simulation *Simu2B* with an ionizing source providing the same UV flux ($\lambda < 912$ Å). We include hot stellar winds, consider a dense halo environment, and the photoionization rate of our source is 2.43×10^{47} s^{-1}.

As expected, the results are similar to the ones of *Simu2B*, i.e. temperature and density profile, as well as the gas mass accumulated in the stellar cluster (Figs 3 and 5). This is due to the fact that both ionizing photons rates used here (2.43×10^{47} and 5.7×10^{48} s^{-1}) are already a few orders of magnitude higher than the rate needed to fully ionize the ICM (1.6×10^{44} photons s^{-1} with wavelengths < 912 Å, McDonald & Zijlstra 2015).

4 DISCUSSION

We investigate stellar clusters of 10^5 and 10^6 $M_\odot$, with and without ram pressure stripping as well as photoionization. We find that for most cases, the ram-pressure stripping alone is not enough to effectively remove the ICM from the clusters due to the fact that the gas concentrates in the central regions of the clusters (due to cooling). However, when including photoionization, the gas is heated and expands to fill the full volume of the cluster (i.e. not concentrate in the cluster centre). Due to this increased surface area, the ICM can then be more efficiently stripped by ram pressure, this mechanism working on very short time-scales ($\lesssim$3 Myr).

Our simulations with ram pressure and without photoionization showed that globular clusters with masses around 10^5 $M_\odot$ display in general a low ICM in their centre. For more massive GCs ($\sim 10^6$ $M_\odot$), the ram-pressure mechanism alone is not efficient enough to strip the ICM even in a dense environment (i.e. GCs orbiting within $\sim$10 kpc from the Galactic centre). However, the addition of ionization by UV sources provide a UV flux ($\lambda < 912$ Å) able to fully ionize the cluster's ICM and favour its loss.

Most of typical intermediate-mass GCs should also host a source with a photon rate high enough to ionize their ICM, then favouring its loss (similar to what happens in massive GCs to a lesser extent). Thus, if we take into account ram-pressure stripping and ionization, we predict a negligible ICM within these typical GCs and the values reported in Table 3 (taking into account only ram-pressure stripping) are upper limits.

On the other hand, while taking into account ram-pressure stripping and ionization, massive GCs will display a low amount of ionized ICM in their central region, in agreement with observations.

To summarize, we do not expect to find any significant ionized ICM in the core of globular clusters, regardless of their mass and their distance to the Galactic centre. However, this very low amount of ionized ICM should be detectable inside the core of massive GCs ($M \gtrsim 5 \times 10^5$ $M_\odot$). These predictions can be tested by investigating the total ICM within the inner 5 pc of the most massive GCs, such as 47 Tuc, NGC 2419, NGC 2808, NGC 5139, NGC 5824, NGC 6266, NGC 6273, NGC 6284, Liller 1, NGC 6388, NGC 6402, Terzan 5, NGC 6441, NGC 6715, NGC 6864, and NGC 7089.

The same mechanisms presented in this work could also be efficient at younger ages. Therefore, in a future work we will extend our simulations to study the early phases of young massive clusters (YMCs) and proto-GCs.

We have shown that without photoionization, the gas cools and sinks to the centre, which minimizes its cross-sectional area, and in turn, minimizes the effect of ram pressure. This result has strong implications on scenarios trying to explain the origin and formation of multiple stellar populations within GCs. Indeed, some of these scenarios require that the gas in stellar clusters is retained for a non-negligible period of time and be allowed to cool to form these different stellar generations (e.g. D'Ercole et al. 2008). For instance in the AGB scenario, the second stellar population starts to form after the explosion of all type II SNe of the first stellar population at about 40 Myr and it lasts until $\sim$100 Myr.

During the early evolution of the progenitor of globular clusters, the properties of the environment are expected to be different. In addition, the stellar population of these very young clusters will provide a strong UV flux. Thus, it is vital while investigating the early evolution of the ICM in GC progenitors and the formation of multiple populations to take into account the radiative feedback effects of stars (see also Conroy & Spergel 2011). For instance, if all the ionizing sources of the stellar cluster are not taken into account and the full radiative transfer calculations are not included in the simulations on the formation of multiple populations, it might greatly favour the formation of the second stellar population in the

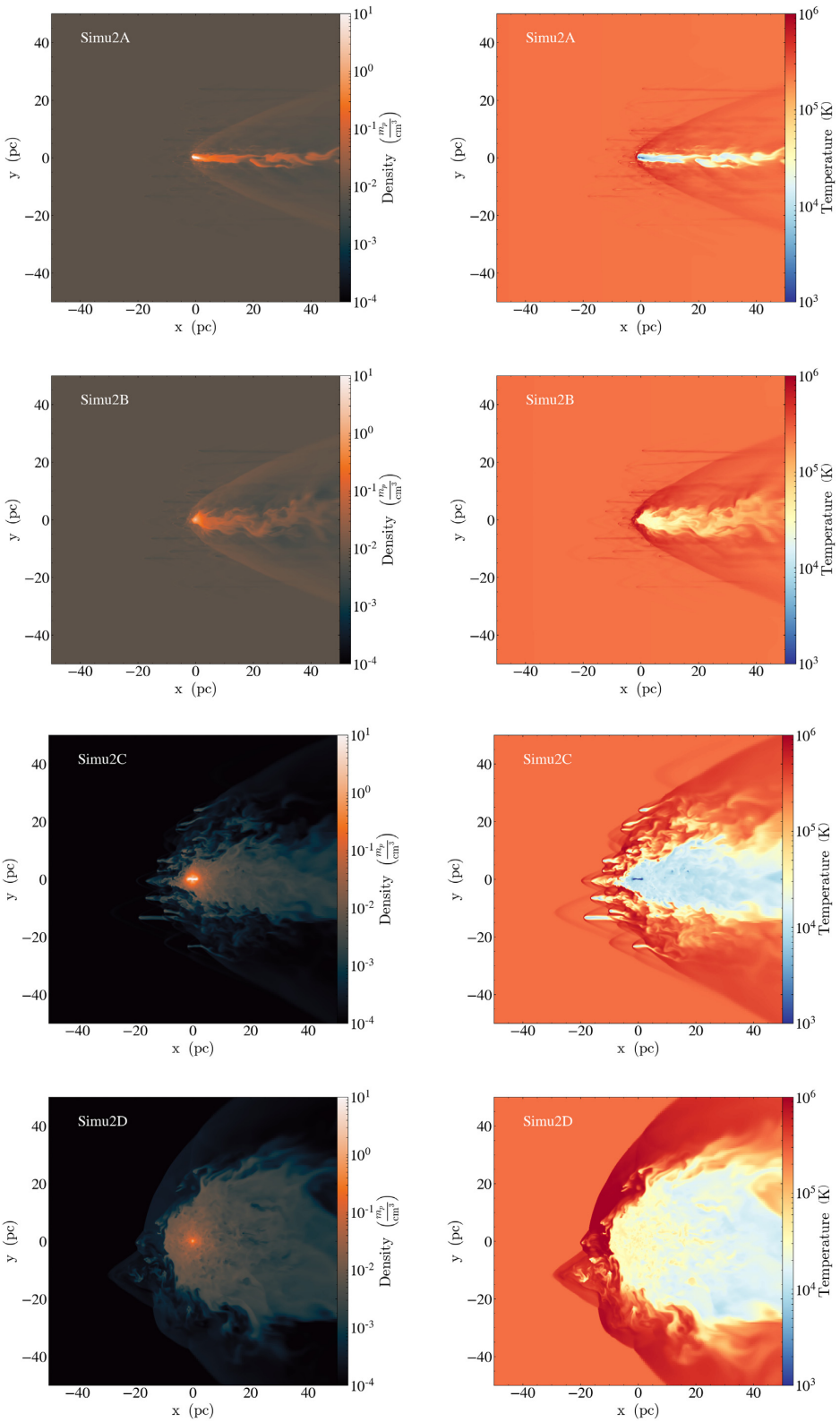

Figure 4. Snapshots at 5 Myr displaying the density (left) and temperature (right) maps of simulations *Simu2A*, *Simu2B*, *Simu2C*, and *Simu2D*.

centre of the cluster due to the cooling and sinking gas (D'Ercole, D'Antona & Vesperini 2016; Calura et al. 2019).

Bastian, Hollyhead & Cabrera-Ziri (2014), Hollyhead et al. (2015), Cabrera-Ziri et al. (2015), and Hannon et al. (2019) have found that YMCs were gas free within the first 2–4 Myr of their lives. Thus, these stellar clusters are very efficient at clearing out their gas, at odds with theoretical studies without invoking special circumstances (e.g. IMF variations, high star formation efficiency,

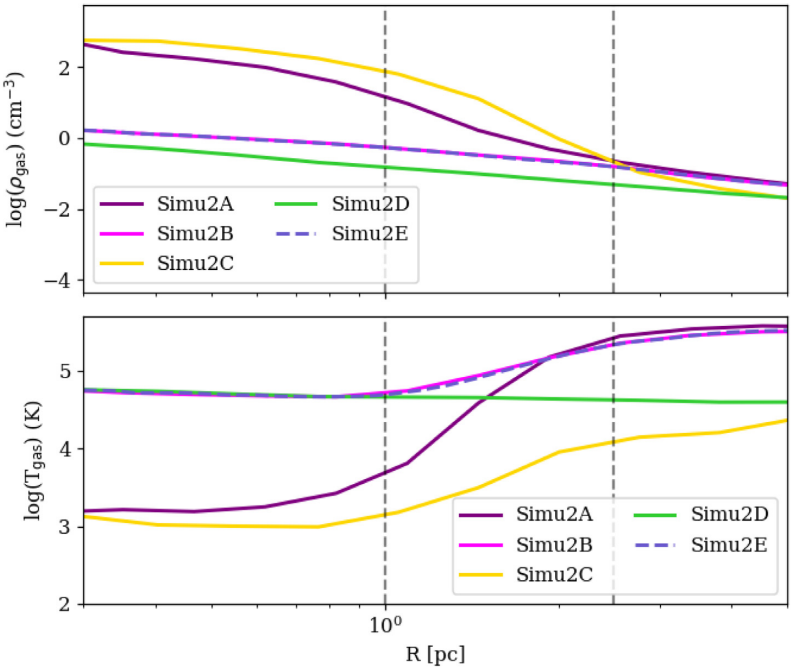

Figure 5. Density (top) and temperature profiles (bottom) for *Simu2A*, *Simu2B*, *Simu2C*, *Simu2D*, and *Simu2E* at 5 Myr. The dashed vertical lines correspond to radii of 1 and 2.5 pc, respectively.

strong coupling of the energy produced by stellar feedback to the gas, Krause et al. 2016). The results of this study suggest that the combined effect of radiative heating and radiative pressure (from ionizing sources) with ram-pressure stripping could be the processes at work in YMCs, which would explain why they are gas free.

ACKNOWLEDGEMENTS

WC acknowledges funding from the Swiss National Science Foundation under grant P400P2_183846. PB acknowledges ERC starting grant 638707. NB and WC gratefully acknowledge financial support from the European Research Council (ERC-CoG-646928, Multi-Pop). NB gratefully acknowledges financial support from the Royal Society (University Research Fellowship). We would like to thank Iain Mcdonald, Joki Rosdahl, and Maxime Trebitsch for useful discussions. This research used: The Cambridge Service for Data Driven Discovery (CSD3), part of which is operated by the University of Cambridge Research Computing on behalf of the STFC DiRAC HPC Facility (www.dirac.ac.uk). The DiRAC component of CSD3 was funded by BEIS capital funding via STFC capital grants ST/P002307/1 and ST/R002452/1 and STFC operations grant ST/R00689X/1. The DiRAC@Durham facility managed by the Institute for Computational Cosmology on behalf of DiRAC. The equipment was funded by BEIS capital funding via STFC capital grants ST/P002293/1 and ST/R002371/1, Durham University, and STFC operations grant ST/R000832/1. DiRAC is part of the National eInfrastructure. Finally, we would like to thank the referee for the pertinent questions, and suggestions that have greatly helped us improve the presentation of our results.

REFERENCES

Abbate F., Possenti A., Ridolfi A., Freire P. C. C., Camilo F., Manchester R. N., D'Amico N., 2018, MNRAS, 481, 627
Barmby P., Boyer M. L., Woodward C. E., Gehrz R. D., van Loon J. T., Fazio G. G., Marengo M., Polomski E., 2009, AJ, 137, 207
Bastian N., Hollyhead K., Cabrera-Ziri I., 2014, MNRAS, 445, 378
Baumgardt H., Hilker M., 2018, MNRAS, 478, 1520
Boyer M. L., Woodward C. E., van Loon J. T., Gordon K. D., Evans A., Gehrz R. D., Helton L. A., Polomski E. F., 2006, AJ, 132, 1415
Boyer M. L., McDonald I., van Loon J. T., Woodward C. E., Gehrz R. D., Evans A., Dupree A. K., 2008, AJ, 135, 1395
Cabrera-Ziri I. et al., 2015, MNRAS, 448, 2224
Calura F., D'Ercole A., Vesperini E., Vanzella E., Sollima A., 2019, MNRAS, 489, 3269
Coleman G. D., Worden S. P., 1977, ApJ, 218, 792
Conroy C., Spergel D. N., 2011, ApJ, 726, 36
D'Ercole A., Vesperini E., D'Antona F., McMillan S. L. W., Recchi S., 2008, MNRAS, 391, 825
D'Ercole A., D'Antona F., Vesperini E., 2016, MNRAS, 461, 4088
de Boer T. J. L., Gieles M., Balbinot E., Hénault-Brunet V., Sollima A., Watkins L. L., Claydon I., 2019, MNRAS, 485, 4906
Dupree A. K., Smith G. H., Strader J., 2009, AJ, 138, 1485
Evans A., Stickel M., van Loon J. T., Eyres S. P. S., Hopwood M. E. L., Penny A. J., 2003, A&A, 408, L9
Frank J., Gisler G., 1976, MNRAS, 176, 533
Freire P. C., Kramer M., Lyne A. G., Camilo F., Manchester R. N., D'Amico N., 2001, ApJ, 557, L105
Gavagnin E., Bleuler A., Rosdahl J., Teyssier R., 2017, MNRAS, 472, 4155
Geen S., Hennebelle P., Tremblin P., Rosdahl J., 2015, MNRAS, 454, 4484
Gieles M., Zocchi A., 2015, MNRAS, 454, 576
Gillett F. G., de Jong T., Neugebauer G., Rice W. L., Emerson J. P., 1988, AJ, 96, 116
Groenewegen M. A. T., 2014, A&A, 561, L11
Hannon S. et al., 2019, MNRAS, 490, 4648
Hollyhead K., Bastian N., Adamo A., Silva-Villa E., Dale J., Ryon J. E., Gazak Z., 2015, MNRAS, 449, 1106
King I. R., 1966, AJ, 71, 64
Krause M. G. H., Charbonnel C., Bastian N., Diehl R., 2016, A&A, 587, A53
Lagarde N., Decressin T., Charbonnel C., Eggenberger P., Ekström S., Palacios A., 2012, A&A, 543, A108

Matsunaga N. et al., 2008, PASJ, 60, S415
Mauas P. J. D., Cacciari C., Pasquini L., 2006, A&A, 454, 609
McDonald I., van Loon J. T., 2007, A&A, 476, 1261
McDonald I., Zijlstra A. A., 2015, MNRAS, 446, 2226
Mészáros S., Avrett E. H., Dupree A. K., 2009, AJ, 138, 615
Miller M. J., Bregman J. N., 2013, ApJ, 770, 118
Moore K., Bildsten L., 2011, ApJ, 728, 81
Netzer N., Elitzur M., 1993, ApJ, 410, 701
Odenkirchen M., Brosche P., Geffert M., Tucholke H.-J., 1997, New Astron., 2, 477
Priestley W., Ruffert M., Salaris M., 2011, MNRAS, 411, 1935
Reimers D., 1975, Mem. Soc. R. Sci. Liege, 8, 369
Roberts M. S., 1988, in Grindlay J. E., Philip A. G. D., eds, Proc. IAU Symp. 126, The Harlow-Shapley Symposium on Globular Cluster Systems in Galaxies. Kluwer, Dordrecht, p. 411
Rosdahl J., Teyssier R., 2015, MNRAS, 449, 4380
Rosdahl J., Blaizot J., Aubert D., Stranex T., Teyssier R., 2013, MNRAS, 436, 2188
Rosdahl J., Schaye J., Teyssier R., Agertz O., 2015, MNRAS, 451, 34
Salpeter E. E., 1955, ApJ, 121, 161
Scott E. H., Durisen R. H., 1978, ApJ, 222, 612
Smith G. H., Wood P. R., Faulkner D. J., Wright A. E., 1990, ApJ, 353, 168
Spergel D. N., 1991, Nature, 352, 221
Spitzer L., Jr, 1956, ApJ, 124, 20
Sutherland R. S., Dopita M. A., 1993, ApJS, 88, 253
Tayler R. J., Wood P. R., 1975, MNRAS, 171, 467
Taylor J. H., Cordes J. M., 1993, ApJ, 411, 674
Teyssier R., 2002, A&A, 385, 337
Thoul A., Jorissen A., Goriely S., Jehin E., Magain P., Noels A., Parmentier G., 2002, A&A, 383, 491
Umbreit S., Chatterjee S., Rasio F. A., 2008, ApJ, 680, L113
van Loon J. T., Stanimirović S., Evans A., Muller E., 2006, MNRAS, 365, 1277
van Loon J. T., Stanimirović S., Putman M. E., Peek J. E. G., Gibson S. J., Douglas K. A., Korpela E. J., 2009, MNRAS, 396, 1096
Vandenberg D. A., 1978, ApJ, 224, 394
Yokoo T., Fukue J., 1992, PASJ, 44, L253

This paper has been typeset from a TEX/LATEX file prepared by the author.